Lettieri, A., Elettore, E., Pieroni, L., Freddi, F., Latour, M., Rizzano, G. (2022). Parametric Analysis of Steel MRFs with Self-Centring Column Bases. Steel Construction. https://doi.org/10.1002/stco.202100050. Invited paper following the nomination for the Eurosteel 2021 Best Paper Award.

Parametric analysis of steel MRFs with Self-Centring Column Bases

Annarosa Lettieri[1,*], **Elena Elettore**[1], **Ludovica Pieroni**[2], **Fabio Freddi**[2], **Massimo Latour**[1], **Gianvittorio Rizzano**[1]

[1] *Department of Civil Engineering, University of Salerno, Salerno, Italy*
[2]*Department of Civil, Environmental & Geomatic Engineering, University College London, London, UK*
[*]Corresponding Author. *E-mail address:* alettieri@unisa.it

Abstract

In the last few decades, innovative seismic-resilient structural systems have been proposed to reduce the direct and indirect losses related to seismic events. Among others, steel Moment Resisting Frames (MRFs) equipped with Damage-Free Self-Centring Column Bases (SC-CBs) represent a promising solution. Although several configurations of SC-CBs have been proposed in literature, only a few research studies investigated how the significant parameters (*e.g.*, number of storeys, frame layout, seismic mass, seismic intensity) affect the seismic performance of MRFs with SC-CBs. To further investigate this aspect, the present work focuses on the influence of an additional parameter (*i.e.*, the combination of seismic mass and acceleration) on their self-centring capability. Three 5-bays steel MRFs with 4, 6 and 8 storeys are considered as case-study frames and designed based on two different values of the seismic mass (*i.e.*, M1 and M2). Numerical models are developed in OpenSees, Incremental Dynamic Analyses (IDAs) are performed monitoring global Engineering Demand Parameters (EDPs), and fragility curves are derived to evaluate the seismic performance of the structures. It is observed that the inclusion of SC-CBs produces beneficial effects in terms of increased self-centring capability on all the investigated case studies. Moreover, the parametric analysis allows drawing some preliminary observations regarding the influence of the number of stories and seismic mass.

Keywords: Structural Resilience; Steel Moment Resisting Frames; Self-Centring; Damage-free column bases; Residual drifts

1 Introduction

According to modern codes (*e.g.*, [1]-[4]), steel Moment Resisting Frames (MRFs) are designed to experience significant inelastic deformation and damage in case of rare seismic events (*i.e.*, Ultimate Limit State), often leading to significant losses in terms of repair costs and downtime. Among others, inelastic deformations may produce large residual deformations, which may compromise the building's reparability [5]. To overcome these drawbacks, in the last few decades, several research studies focused on the definition of innovative seismic-resilient structures capable of sustaining the design earthquake intensity with low or minimal damage and return to the undamaged, fully functional condition in a short time (*e.g.*, [6]-[8]). In this context, MRFs equipped with Self-Centring Damage-Free devices at column bases (*e.g.*, [9]) and beam-to-column joints (*e.g.*, [10]-[13]) represent a viable solution to minimise the structural damage and the residual deformations. However, previous studies focused on the widespread use of Self-Centring Damage-Free devices in all the connections with a significant increase of the structures' complexity compared to conventional systems, thus limiting their application in practice. To overcome this drawback, current research works are focusing on the use of Self-Centring Damage-Free devices only at some 'key' locations such that their beneficial effect is maximised, and the structural complexity is only slightly increased [14].

Among others, it has been demonstrated that the use of Damage-Free Self-Centring Column Bases (SC-CBs) in conventional MRFs represents an effective solution to minimise the residual drift for low-rise building structures (*e.g.*, [15]-[16]). Most of the SC-CBs investigated in literature are based on a combination of high strength post-tensioned (PT) steel bars (or strands) to promote the self-centring capability of the structure by providing elastic restoring forces to the joints, and dedicated fuses, *e.g.*, Friction Devices (FDs) or yielding devices, to dissipate the seismic input energy. In recent years, several configurations of SC-CBs have been proposed and experimentally investigated (*e.g.*, [17]-[23]). The present study considers the SC-CB developed and experimentally tested by Latour *et al.* [23], which consists of a slotted column splice with a combination of FDs and a system of PT bars and disk springs, as illustrated in Fig. 1. The FDs are composed of friction pads coated with thermally sprayed metal, pre-stressed with high strength bolts and placed between the steel cover plates and the column. The disk springs, arranged in parallel and series, together with the PT bars, act as a macro-spring system, ensuring an adaptable stiffness/resistance combination to the self-centring system. Oversized web holes and flange slots are designed to accommodate the gap opening required to reach the target rotation. The considered SC-CB configuration has the following advantages: *i*) the self-centring capability is obtained with elements, *i.e.*, PT bars and disk springs, which have a size comparable to the overall size of the column (*e.g.*, long PT bars can be avoided); *ii*) the moment-rotation hysteretic behaviour of the components can be easily calibrated; *iii*) all the connection elements are moved far from the concrete foundation, avoiding any interaction with it.

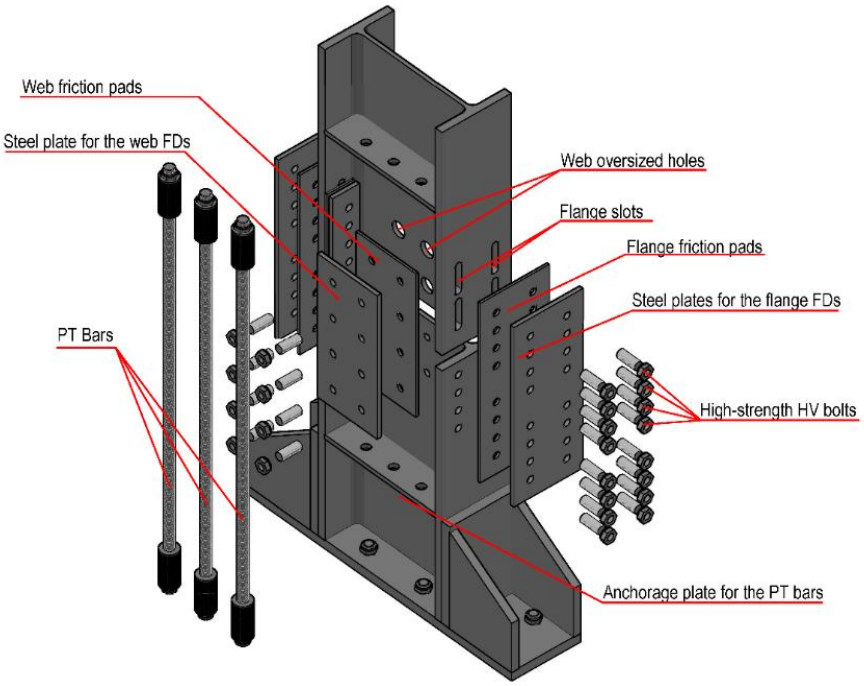

Fig. 1 3D exploded view of the SC-CB connection developed by Latour *et al.* [19].

In the past years, several studies have been developed to investigate the seismic response of steel MRFs equipped with SC-CBs. Considering this type of SC-CBs, Elettore *et al*. [15] numerically investigated the seismic performance of a 3 bay - 4 storey MRF. The study demonstrated that the use of self-centring connections at the column bases represents an effective strategy to reduce the residual drifts of low-rise structures and protect the first storey columns from damage. Although several technologies for SC-CBs have been developed, only a few research studies (*e.g.*, [24]) investigated the influence of the significant parameters (*e.g.*, properties of the SC-CBs, frame layout, number of storeys, seismic inputs) on the effectiveness of these systems in improving the seismic performance (*e.g.*, residual drifts reduction) of the structure. Elettore *et al.* [16] performed a parametric study considering a set of nine case-study buildings with a different number of bays (*i.e.*, 3-, 5-, and 8-bays) and storeys (*i.e.*, 4-, 6- and 8-storeys) to investigate the influence of the frame layout on the self-centring capability of steel MRFs equipped with SC-CBs. This parametric study [16] revealed that the number of storeys significantly affects the self-centring capability of the MRFs with SC-CBs while the differences related to the number of bays are negligible. Within this context, the present work aims to extend the previous results [16] by investigating the influence of an additional parameter (*i.e.*, the variation of seismic mass and/or acceleration) on the self-centring behaviour of MRFs with SC-CBs. Three 5-bays steel MRFs with 4, 6 and 8 storeys are considered as case-study structures, and two different values of the seismic mass (*i.e.*, M1 and M2) are used. The seismic response of conventional MRF (*i.e.*, MRF) and the MRF with SC-CBs (*i.e.*, MRF-CB) are compared. Non-linear Finite Elements (FE) models are developed in OpenSees [25], and Incremental Dynamic Analyses (IDAs) [26] are carried out considering a set of 30 ground motion records accounting for the record-to-record variability. The spectral acceleration corresponding to the fundamental period of vibration is used as Intensity Measure (IM), and global Engineering Demand Parameters (EDPs) are monitored. Fragility curves [27] are successively derived for the residual interstorey drifts. The results show that the use of SC-CBs is beneficial in reducing the residual interstorey drifts for all the investigated case studies. The parametric analysis allows drawing some preliminary observations on the influence of the seismic mass on the use of SC-CBs for the residual drift reduction of steel MRFs.

2 Case-study frames

2.1 Design of the Moment Resisting Frames (MRFs)

Fig. 2 shows the plan and the elevation views of the investigated case-study frames. Two different seismic masses (*i.e.*, M1 and M2) have been adopted considering different tributary areas due to a different number of bays in the *y*-direction, as represented by the hatching areas in Fig. 2(a) (*i.e.*, 3 bays in *y*-direction for M1 and 5-bays in *y*-direction for M2). The seismic resisting system in the *x*-direction is composed of perimeter MRFs, while the interior part is composed of gravity frames. The layout has interstorey heights of 3.20 m except for the first level, whose height is equal to 3.50 m. All the bays have a constant length of 6 m. The present study focuses on the assessment of one perimeter MRFs in the *x*-direction. The MRFs are designed according to Eurocode 8 [1], considering the seismic input based on the product of the seismic mass (M1 or M2) and the corresponding spectral acceleration at the fundamental period of vibration. It is noteworthy that increasing the seismic mass or proportionally increasing the seismic input would generate equivalent results. Hence, despite the analysis being limited to the variation of the seismic mass, similar general results are expected by varying the

seismic input acceleration. For the design purposes, the wind action is considered negligible, and a high seismicity level is assumed for the seismic action. In particular, the Type-1 elastic response spectrum, with a damping factor $\xi = 2\%$, a Peak Ground Acceleration (PGA) equal to 0.35g, and soil type C is considered for the definition of the Design-Based Earthquake (*i.e.*, DBE, Ultimate Limit State - ULS - according to the European definition). The Maximum Credible Earthquake (*i.e.*, MCE, Collapse Limit State - CLS - according to the European definition) is assumed to have an intensity equal to 150% of the DBE. The behaviour factor used for the definition of the design spectrum is equal to q = 6.5, in accordance with Eurocode 8 provisions [1] for MRFs in ductility class high. Steel S275 and S355 are used for beams and columns, respectively. The panel zones are stiffened with doubler plates to ensure adequate overstrength to the joints. The structure has non-structural elements fixed in a way so as not to interfere with structural deformations. Therefore, the interstorey drift limit for the Damage State Limitation (DSL; probability of exceedance of 10% in 10 years) requirements is assumed equal to 1%, as suggested by the Eurocode 8 [1]. It is important to highlight the stiffness requirements related to the DSL control the sizing of beams and columns. Moreover, to compute the interstorey drift demand, a reduction factor ν [1] is assumed equal to 0.5 (the structures belong to class II). The columns' and beams' cross-sections obtained from the design are reported in Fig. 2(b) for all the investigated case studies. Furthermore, Table 1 shows the fundamental periods of vibrations and the Spectral Accelerations corresponding to the DBE ($S_{a,DBE}$) and MCE ($S_{a,MCE}$) for all the case-study buildings. The mass of each storey is evaluated based on the seismic combination of the Eurocode 8 [1] considering the tributary area of the investigated MRFs, *i.e.*, half of the total area as shown in Fig. 2 (a).

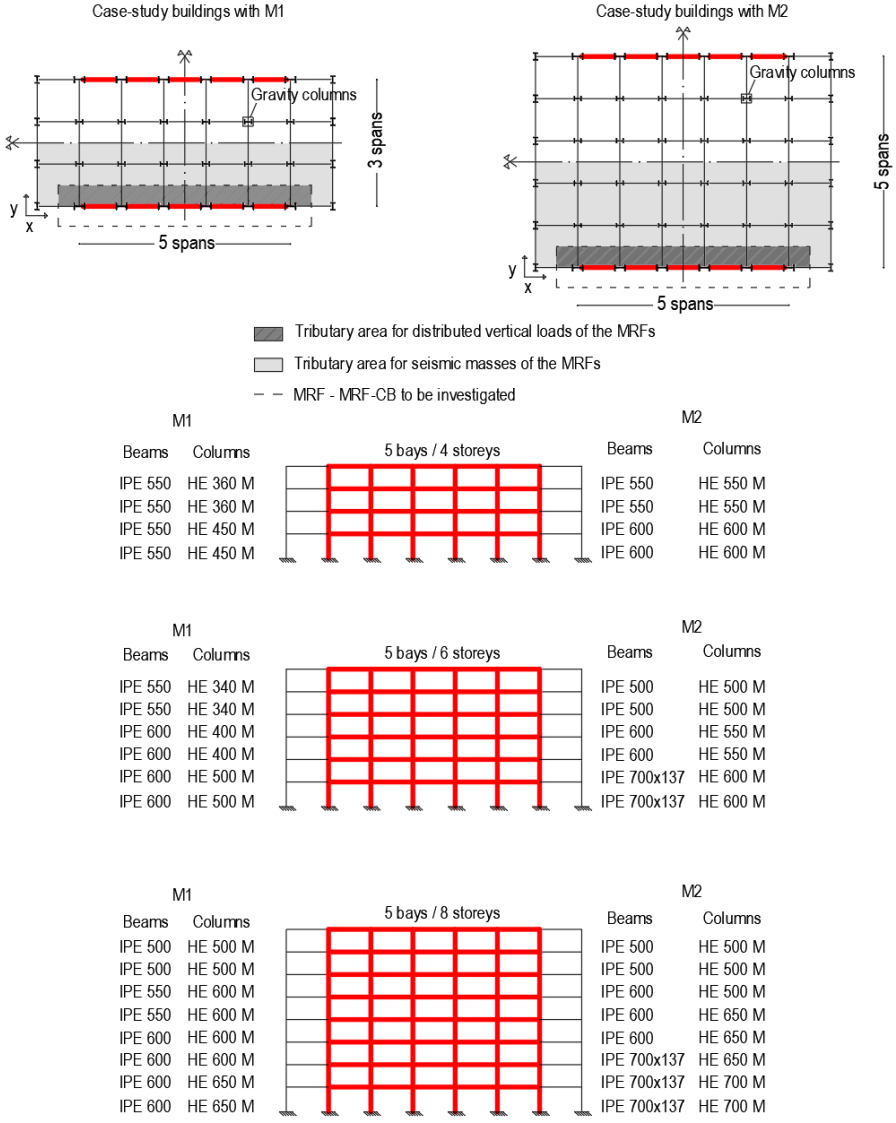

Fig. 2 (a) Plan and (b) elevation views of the case-study buildings.

Table 1 Fundamental period (T_1) and spectral acceleration ($S_a(T_1,\xi)$) for DBE and MCE.

Case-study	T_1 [sec]	$S_{a,DBE}$ [g]	$S_{a,MCE}$ [g]
MRF 5-4 (M1 / M2)	0.72 / 0.74	1.00 / 0.97	1.50 / 1.46
MRF 5-6 (M1 / M2)	0.97 / 1.04	0.74 / 0.70	1.12 / 1.05
MRF 5-8 (M1 / M2)	1.17 / 1.28	0.61 / 0.52	0.92 / 0.79

2.2 Moment-rotation behaviour and design of Self-Centring Column Bases (SC-CBs)

The SC-CB experimentally tested by Latour *et al.* [23] and considered in this paper is characterised by a flag-shape moment-rotation hysteretic behaviour (Fig. 3) which depends on the response of each component (*i.e.*, FDs, PT bars, and disk springs). In Fig. 3(a), F_C represents the compression force at the centre of rotation (COR), F_w and F_f are the sliding forces in the friction pads on the column web and flanges, respectively; F_{PT} is the sum of the initial post-tensioning forces ($F_{PT,0}$), and the additional force consequent to the gap opening while rocking (ΔF_{PT}). N_{Ed}, M_{Ed} and V_{Ed} are the design actions (*i.e.*, axial force, bending moment and shear force) applied to the joint section, h_c is the height of the column section, and t_{fc} is the thickness of the column flange. The flag-shape moment-rotation hysteretic loop is illustrated in Fig. 3(b), where M_D is the decompression moment (*i.e.*, the sum of the moment contributions of the axial force M_N and the moment provided by the PT bars at zero rotation $M_{PT,0}$), while M_{FD} is the moment provided by the FDs. M_1 is the moment that initiates the gap opening, while M_2 is the maximum moment achieved at the design rotation θ_d (*e.g.*, 0.04 rads as suggested by AISC 341-16 [3] for Special Moment Frames). The cyclic moment rotation behaviour can be defined according to the Equations in Fig. 3(b), where K_{eq} is the equivalent axial stiffness of the system of PT bars and disk springs [15] defined as follows:

$$K_{eq} = \frac{K_{PT}K_{ds}}{K_{PT} + K_{ds}}; \qquad K_{PT} = \frac{n_{PT}E_{PT}A_{PT}}{l_{PT}}; \qquad K_{ds} = \frac{n_{ds,par}}{n_{ds,ser}}K_{ds,1};$$

where K_{PT} and K_{ds} are the stiffness of the PT bars and disk spring system respectively, n_{PT} is the number of PT bars in the connection, l_{PT} is the PT bar length including the total length of the disk spring system, $n_{ds,par}$ and $n_{ds,ser}$ are the number of disk springs in parallel and series respectively, and $K_{ds,1}$ is the stiffness of the single disk spring. The design of the proposed SC-CBs is based on the structural analysis of the 'equivalent' MRF. The design values of the axial force N_{Ed} and bending moment M_{Ed} are derived from the amplified combination as required by Eurocode 8 [1]. Conversely, the design shear force is assumed equal to $V_{Ed} = M_{Ed}/L_0$, where L_0 is the shear length. Two main requirements must be satisfied during the design procedure [15]: 1) yielding condition, *i.e.*, the maximum moment in the SC-CB (M_2) must be lower than the yielding moment of the column ($M_{pl,c}$); 2) self-centring condition, *i.e.*, the decompression moment (M_D) should be higher than the moment contribution of the FDs (M_{FD}) to ensure the self-centring behaviour of the connection. It is worth highlighting that: *i*) the columns are characterised by a variability of the axial force, due to the dynamic overturning effects of seismic action, *ii*) M_2 and M_D are strongly affected by the axial force (N_{ed}) happening at the base of the columns. Therefore, for each column, the two design requirements are performed for both the maximum and minimum axial forces. In particular, the maximum axial force represents the 'worst' condition for the no yielding requirement, while the minimum axial force is the 'worst' condition for the self-centring requirement. Based on these considerations, two different configurations are designed for SC-CBs applied to internal and external columns subjected respectively to low and high axial force variability. The friction pads consist of 8 mm of thermally sprayed friction metal steel shims with friction coefficient equal to $\mu = 0.53$, chosen according to the results of previous tests carried out by Cavallaro *et al.* [28]. The bolts for the FDs are HV M30 10.9 class; the PT bars are high-strength M36 10.9 class with a maximum post-tensioning capacity of 514 kN, while the resistance and stiffness (K_{ds1}) of each disk spring are 200 kN and 100 kN/mm, respectively. Table 2 summarises the main components of the SC-CBs (*i.e.*, number and the pre-load force in the bolts of the FDs and in the PT bars of the internal and external columns).

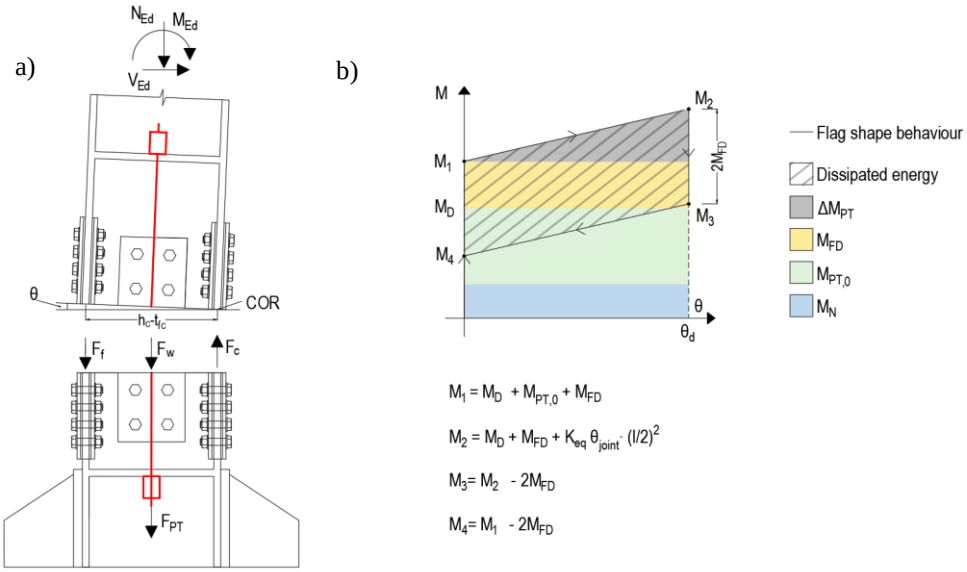

Fig. 3 (a) Schematic representation of the expected forces among the components during rocking; (b) Theoretical moment-rotation hysteretic curve.

Table 2 Components of the SC-CBs.

Case-study	Number of PT Bars [-]	Number of web bolts [-] (Pre-load web bolts [kN])	Number of flange bolts [-] (Pre-load flange bolts [kN])
		External columns	
MRF 5-4 (M1 / M2)	8 / 8	4 (120) / 4 (164)	8 (105) / 4 (205)
MRF 5-6 (M1 / M2)	8 / 8	4 (130) / 4 (170)	8 (120) / 4 (230)
MRF 5-8 (M1 / M2)	8 / 10	4 (135) / 4 (179)	8 (135) / 4 (183)
		Interior columns	
MRF 5-4 (M1 / M2)	6 / 6	4 (125) / 4 (202)	8 (120) / 4 (178)
MRF 5-6 (M1 / M2)	6 / 4	4 (165) / 4 (215)	8 (100) / 4 (225)
MRF 5-8 (M1 / M2)	6 / 4	4 (170) / 4 (225)	8 (80) / 4 (218)

2.3 Moment Resisting Frame (MRF) and Self-Centring Column Base (SC-CB) modelling

As only one the perimeter MRFs in the *x*-direction is considered as a case-study structure, two-dimensional FE models of the MRFs and MRF-CBs are developed in OpenSees [25] for all the case studies. Beams are modelled using a lumped plasticity approach with plastic hinges implemented as suggested by Lignos and Krawinkler [29]. Conversely, columns are modelled with a distributed plasticity approach to capture the axial force-bending moment interaction. The '*Scissor*' model [30] is used to model the panel zone stiffness and strength. Additionally, a leaning column is included to consider the P-Δ effects related to the gravity frames [31]. Gravity loads are applied on the beams by considering the seismic combination for the ULS in Eurocode 8 [1], while the masses are concentrated at the beam-to-column intersections considering the tributary areas of the MRFs shown in Fig. 2(a). Damping sources other than the hysteretic energy dissipation are modelled through a Rayleigh damping factor of 2% for the first two vibration modes. The SC-CBs connections are implemented by following the strategy proposed by Elettore *et al*. [15]. FDs are modelled with zero-length elements with the '*Steel01*' material [25] to simulate the bilinear hysteretic response. Conversely, the rocking behaviour is modelled with zero-length elements with the '*ENT*' material [25] to model the contact behaviour. The self-centring system is implemented with a central zero-length translational spring with bilinear elastic-plastic behaviour, with the '*Initial strain material*' [25], to reproduce the initial post-tensioning force of the PT bars.

3 Performance-based assessment of the case-study frames

3.1 Ground motion selection

Incremental Dynamic Analyses (IDAs) [26] have been carried out to investigate the seismic performances of MRFs and MRF-CBs for the six case-study frames. A suite of 30 ground motion records is selected from SIMBAD Database using REXEL [32] to account for the record-to-record variability. For each case study, a set of ground motion records is selected with the following parameters: moment magnitude (M_w) ranging from 6 to 7, epicentral distance $R \leq 30$ km, and spectrum-compatibility in the range of periods between $0.2T_1$ and $2T_1$, where T_1 is the fundamental period of the structure. The mean elastic spectrum of the records is kept between 75% and 130% of the corresponding Eurocode 8 based elastic response spectrum [1] considered for the design, assumed as target reference spectrum respect to which the compatibility has to be accomplished.

The spectral acceleration corresponding to the first vibration mode ($S_a(T_1,\xi)$) is used as IM. It is worth underlining that for all the case studies, the conventional MRFs and the MRF-CBs have the same fundamental vibration period (T_1) and hence the same values of IM (see Table 1), allowing the comparison of the fragility curves.

3.2 Incremental Dynamic Analyses (IDAs)

Peak and residual interstorey drifts are used to monitor the seismic performances of the case-studies investigated. The maximum values of these quantities among all the storeys are used as global EDPs (*i.e.*, $\theta_{max\text{-}peak}$ and $\theta_{max\text{-}res}$). The effectiveness of the SC-CBs in reducing the residual interstorey drifts is evaluated by the comparison between the seismic response of the MRF and the MRF-CB.

Fig. 4(a) and (b) show the results of the IDAs for the maximum (among all the storeys) peak interstorey drifts ($\theta_{max\text{-}peak}$) for the 6-storeys case-study structures with mass M1 and M2, respectively. Similar results are observed for the other case studies, which, for the sake of brevity, are not reported here. As expected from the design, the requirements for the Frequently Occurred Earthquake (*i.e.*, FOE, Damage Limit State - DLS - according to the European definition) lead to similar $\theta_{max\text{-}peak}$ results for M1 and M2. Additionally, Fig. 4 also shows that the MRFs and MRF-CB experience similar values of $\theta_{max\text{-}peak}$.

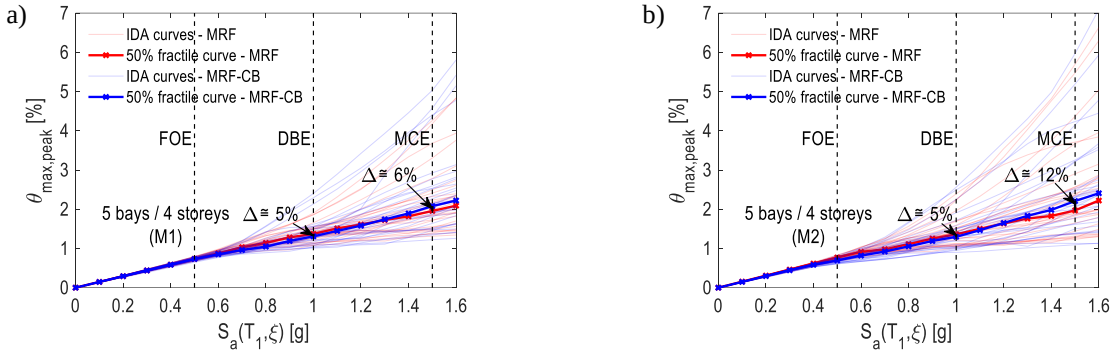

Fig. 4 IDAs Results. Comparison of the maximum peak interstorey drifts for (a) 5-4 (M1); (b) 5-4 (M2).

Fig. 5 shows the results of the IDAs in terms of maximum (among all the storey) residual interstorey drift ($\theta_{max\text{-}res}$) for all the investigated structures. The value $\theta_{max\text{-}res}$ = 0.5% is assumed as the threshold beyond which repairability is not economically viable [5]. In Fig. 5, each row refers to a case study structure with the same number of stories for M1 (left) and M2 (right). Each figure shows IDA curves for all the ground motions for the MRFs (red lines) and the MRF-CBs (blue lines). Additionally, the median value of $\theta_{max\text{-}res}$ among all ground motions (*i.e.*, 50% percentile) is shown for both MRFs and MRF-CBs (bold red and blue lines). The results show that the inclusion of SC-CBs produces beneficial effects in all cases allowing a residual drift reduction for both M1 and M2 for all the IM values. Additionally, in all cases, the use of SC-CBs allows reducing the median values of $\theta_{max\text{-}res}$ below the assumed repairability threshold (*i.e.*, 0.5%) for all the investigated IM values. Conversely, all the conventional MRFs with both M1 and M2 do not satisfy this limit for high IM values. Fig. 5 shows minor differences in terms of residual drifts reduction between the cases with M1 and M2.

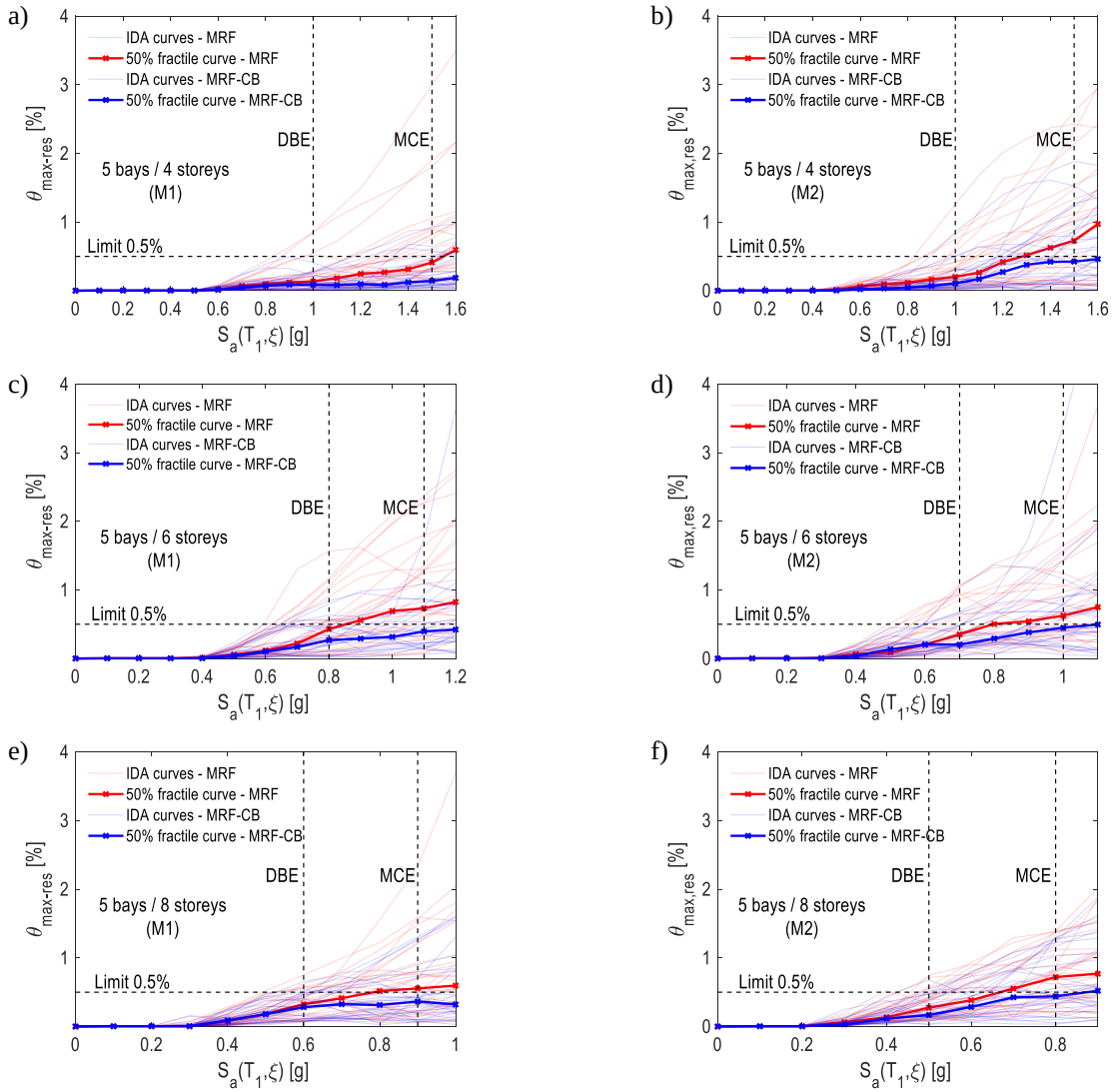

Fig. 5 IDAs Results. Comparison of the maximum residual interstorey drifts for the case-study frames: (a) 5-4 (M1); (b) 5-4 (M2); (c) 5-6 (M1); (d) 5-6 (M2); (e) 5-8 (M1); (f) 5-8 (M2).

3.3 Fragility curves

Fragility curves [33] are used to quantify the probability of the maximum residual interstorey drifts (*i.e.*, $\theta_{max\text{-}res}$) exceeding the associated threshold equal to 0.5% for each IM value (*i.e.*, P_f). Numerical fragility curves are initially derived based on EDPs-IMs pairs obtained through IDAs and successively fitted by analytical lognormal curves through least-square minimisation. The comparison of the fragility curves is represented in Fig. 6 where each row refers to a case study structure with the same number of stories for M1 (left) and M2 (right), and the figures show the comparison between the MRFs (red line) and the MRF-CBs (blue line). Additionally, the percentage reduction of the probability of exceeding the limit value (*i.e.*, ΔP_f) is reported for the two seismic intensities of interest (*i.e.*, DBE and MCE). The fragility curves confirm the beneficial effect of the SC-CBs in reducing the residual interstorey drifts for the whole range of IM values of interest, *i.e.*, the MRF-CBs experience lower values of P_f with respect to the MRF for all IM values. It can be observed that the 4-storey case study with M1 shows the highest beneficial effects (*i.e.*, the highest ΔP_f) of the use of SC-CBs in reducing the residual interstorey drifts. The results show that this difference progressively decreases in the 6- and 8-storey case studies, as previously observed by Elettore *et al.* [16]. Conversely, it can be observed that the higher mass value M2, results in a lower but more uniform and less sensitive from the number of stories, the effectiveness of the SC-CBs in reducing the residual interstorey drifts.

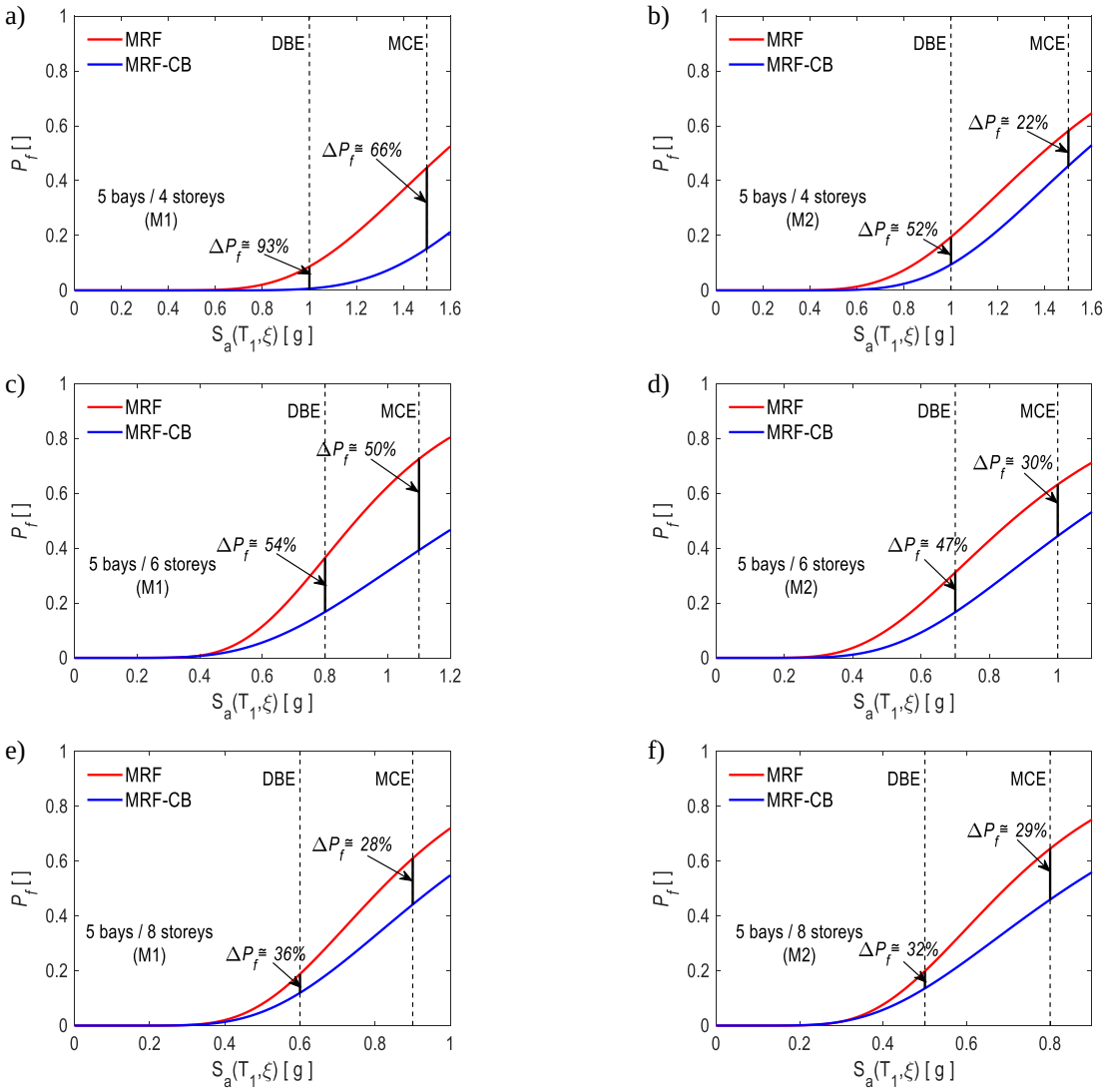

Fig. 6 Comparison of the fragility curves for themaximum residual interstorey drifts for the case-study frames: (a) 5-4 (M1); (b) 5-4 (M2); (c) 5-6 (M1); (d) 5-6 (M2); (e) 5-8 (M1); (f) 5-8 (M2).

4 Conclusions

The present study investigates the influence of the seismic mass and/or spectral acceleration on the self-centring capability of steel Moment Resisting Frames (MRFs) equipped with the Damage-Free Self-Centring Column Bases (SC-CBs). Three 5-bays steel MRFs with 4, 6 and 8 storeys are considered as case-study frames and designed based on two different values of the seismic mass (*i.e.*, M1 and M2). For each case study, the conventional MRF and the MRF with SC-CBs are designed, and their seismic responses are compared. Non-linear finite element models of the MRF and MRF with SC-CBs are developed in OpenSees, and Incremental Dynamic Analyses are carried out with a set of 30 ground motion records

accounting for the record-to-record variability. The spectral acceleration corresponding to the fundamental period of vibration is used as Intensity Measure (IM), and the peak and residual interstorey drifts are monitored as global Engineering Demand Parameters (EDPs). Fragility curves are successively derived to evaluate the self-centring capability of the structures. The results show the beneficial effect of the SC-CBs in reducing the residual interstorey drifts for all the case study structures and the whole range of IM values of interest. For the lower mass M1, it can be observed that the effectiveness progressively decreases while increasing the number of stories, as observed in previous studies. Conversely, for the higher mass M2, the results show to be less sensitive to the number of stories. The results herein presented refer to the investigated case-study frames. Additional research studies are needed to provide a more general understanding of the influence of the investigated parameters on the self-centring capability of steel MRF with SC-CBs.

References

[1] EN 1998-1 (2004) *Eurocode 8: Design of structures for earthquake resistance – Part 1: General rules, seismic actions and rules for buildings*, European Committee for Standardization, Brussels.

[2] ASCE/SEI 7-16 (2017) *Minimum design loads and associated criteria for buildings and other structures*, American Society of Civil Engineers, Reston, USA.

[3] ANSI/AISC 341-16 (2016) *Seismic provisions for structural steel buildings*, American Institute of Steel Construction, Chicago, USA.

[4] Gutiérrez-Urzúa, L.F., Freddi, F., Di Sarno, L. (2021). *Comparative Analysis of Code Based Approaches for the Seismic Assessment of Existing Steel Moment Resisting Frames*, Journal of Constructional Steel Research, 181: 106589.

[5] McCormick, J., Aburano, H., Nakashima, M. (2008) *Permissible residual deformation levels for building structures considering both safety and human elements*, 14th World Conference on Earthquake Engineering (WCEE), October 12-17, Beijing, China.

[6] Chancellor NB, Eatherton MR, Roke DA, Akbas T. (2014) *Self-Centering Seismic Lateral Force Resisting Systems: High Performance Structures for the City of Tomorrow*, Buildings, 4: 520–548.

[7] Dall'Asta A, Leoni G., Micozzi F., Gioiella L., Ragni L. (2020). *A resilience and robustness oriented design of base-isolated structures: the new Camerino University Research Center*, Frontiers in Built Environment, 6: 50. https://doi.org/10.3389/fbuil.2020.00050.

[8] Freddi, F., Galasso, C., Cremen, G., Dall'Asta, A., Di Sarno, L., Giaralis, A., Gutiérrez-Urzúa, L.F., Málaga-Chuquitaype, C., Mitoulis S., Petrone, C., Sextos, A., Sousa, L., Tarbali, K., Tubaldi, E., Wardman, J., Woo, G. (2021) *Innovations in Earthquake Risk Reduction for Resilience: Recent Advances and Challenges*, International Journal of Disaster Risk Reduction, 60: 102267. https://doi.org/10.1016/j.ijdrr.2021.102267.

[9] Kamperidis, V.C., Karavasilis, T.L., Vasdravellis, G. (2018), *Self-centring steel column base with metallic energy dissipation devices*, Journal of Constructional Steel Research, 149: 14-30.

[10] Ricles, J.M., Sause, R., Garlock, M. (2001) *Posttensioned Seismic-Resistant Connections for Steel Frames*, Journal of Structural Engineering, 127(2): 113–121.

[11] Garlock, M., Sause, R., Ricles, J.M. (2007) *Behavior and Design of Posttensioned Steel Frame Systems*, Journal of Structural Engineering, 133(3): 389-399.

[12] Karavasilis, T.L., Seo C-Y. (2011) *Seismic structural and non-structural performance evaluation of highly damped self-centering and conventional systems*, Engineering Structures, 33: 2248-2258.

[13] Dimopoulos, C., Freddi, F., Karavasilis, T.L., Vasdravellis, G. (2020). *Progressive collapse of Self-Centering moment resisting frames*. Engineering Structures, 208: 109923. DOI: doi.org/10.1016/j.engstruct.2019.109923.

[14] Pieroni, L., Freddi, F., Latour, M. (2022) *Effective placement of Self-Centering Damage-Free Connections for Seismic-Resilient Steel Moment Resisting Frames*, Earthquake Engineering and Structural Earthquake, 51: 1292–1316. https://doi.org/10.1002/eqe.3615.

[15] Elettore, E., Freddi, F., Latour, M., Rizzano, G. (2020) *Design and analysis of a seismic resilient steel moment resisting frame equipped with damage free self-centring column bases*, Journal of Constructional Steel Research, 179: 106543.

[16] Elettore, E., Lettieri, A., Freddi, F., Latour, M., Rizzano G. (2021) *Performance-Based Assessment of Seismic-Resilient Steel Moment Resisting Frames Equipped with Innovative column Bases Connections*, Structures, 32: 1646-1664.

[17] Takamatsu, T., Tamai, H. (2005) *Non-slip-type restoring force characteristics of an exposed-type CB*, Journal of Constructional Steel Research; 61(7): 942–961.

[18] Ikenaga, M., Nagae, T., Nakashima, M., Suita, K. (2006) *Development of CBs having self-centering and damping capability*. 5th International Conference on Behaviour of Steel Structures in Seismic Areas, Yokohama, Japan.

[19] Chou, CC., Chen, JH. (2011) *Analytical model validation and influence of CBs for seismic responses of steel post-tensioned self-centering MRF systems*, Engineering Structures; 33(9): 2628–2643.

[20] Chi, H., Liu, J. (2012) *Seismic behaviour of post-tensioned CB for steel self-centering moment resisting frame*, Journal of Constructional Steel Research; 78: 117–130.

[21] Freddi, F., Dimopoulos, CA., Karavasilis, TL. (2017) *Rocking damage-free steel CB with Friction Devices: design procedure and numerical evaluation*, Earthquake Engineering and Structural Dynamics; 46: 2281–2300.

[22] Freddi, F., Dimopoulos, CA., Karavasilis, TL. (2020) *Experimental evaluation of a rocking damage-free steel CB with friction devices*, Journal of Structural Engineering. (ASCE); 146(10): 04020217. doi: 10.1061/(asce)st.1943-541x.0002779.

[23] Latour, M., Rizzano, G., Santiago, A., Da Silva, L. (2019) *Experimental response of a low-yielding, self-centering, rocking CB joint with friction dampers*, Soil Dynamics and Earthquake Engineering; 116: 580–592.

[24] Herning, G., Garlock, MEM., Vanmarcke, E. (2011) *Reliability-based evaluation of design and performance of steel self-centring moment frames*, Journal of Constructional Steel Research; 67: 1495–1505.

[25] Mazzoni, S., McKenna, F., Scott, MH., Fenves, GL. (2009) *OpenSEES: Open System for earthquake engineering simulation*, Pacific Earthquake Engineering Research Centre (PEER), University of California, Berkley, CA, Available at: http://opensees.berkeley.edu.

[26] Vamvatsikos, D., Cornell, CA. (2002) *Incremental Dynamic Analysis*, Earthquake Engineering and Structural Dynamics; 31(3): 491–514.

[27] Shinozuka, M., Feng, MQ., Kim, H-K., Kim, S-H. (2000) *Non-linear static procedure for fragility curve development*, Journal of Engineering Mechanics; 126(12): 1287–95.

[28] Cavallaro, GF., Francavilla, A., Latour, M., Piluso, V., Rizzano, G. (2008) *Cyclic behaviour of friction materials for low yielding connections*. Soil Dynamics and Earthquake Engineering; 114: 404–423.

[29] Lignos, D., Krawinkler, H., (2011) *Deterioration Modelling of Steel Components in Support of Collapse Prediction of Steel Moment Frames under Earthquake loading*, Journal of Structural Engineering; 137: 1291–1302.

[30] Charney, F., Downs, W., (2004) *Modelling procedures for panel zone deformations in moment resisting frames*. Connections in Steel Structures; ESSC/AISC Workshop, Amsterdam.

[31] Foutch, DA., Yun, S-Y., (2002) *Modeling of steel moment frames for seismic loads*, Journal of Constructional Steel Research; 58: 529–564.

[32] Iervolino, I., Galasso, C., Cosenza, E., *REXEL: Computer aided record selection for code-based seismic structural analysis*, Bulletin of Earthquake Engineering; 8: 339-362.

[33] Cornell, CA., Jalayer, F., Hamburger, RO., Foutch, DA. (2002) *Probabilistic Basis for 2000 SAC Federal Emergency Management Agency Steel Moment Frame Guidelines*. Journal of Structural Engineering; 128:526-533.